

DESY 11-173
December 2011

Predicting θ_{13} and the Neutrino Mass Scale from Quark Lepton Mass Hierarchies

W. Buchmüller, V. Domcke, and K. Schmitz

Deutsches Elektronen-Synchrotron DESY, 22607 Hamburg, Germany

Abstract

Flavour symmetries of Froggatt-Nielsen type can naturally reconcile the large quark and charged lepton mass hierarchies and the small quark mixing angles with the observed small neutrino mass hierarchies and their large mixing angles. We point out that such a flavour structure, together with the measured neutrino mass squared differences and mixing angles, strongly constrains yet undetermined parameters of the neutrino sector. Treating unknown $\mathcal{O}(1)$ parameters as random variables, we obtain surprisingly accurate predictions for the smallest mixing angle, $\sin^2 2\theta_{13} = 0.07_{-0.05}^{+0.11}$, the smallest neutrino mass, $m_1 = 2.2_{-1.4}^{+1.7} \times 10^{-3}$ eV, and one Majorana phase, $\alpha_{21}/\pi = 1.0_{-0.2}^{+0.2}$.

arXiv:1111.3872v3 [hep-ph] 7 Mar 2012

1 Introduction

It remains a theoretical challenge to explain the observed pattern of quark and lepton masses and mixings, in particular the striking differences between the quark sector and the neutrino sector. Promising elements of a theory of flavour are grand unification (GUT) based on the groups $SU(5)$, $SO(10)$ or E_6 , supersymmetry, the seesaw mechanism and additional flavour symmetries [1]. A successful example is the Froggatt-Nielsen mechanism [2] based on spontaneously broken Abelian symmetries, which parametrizes quark and lepton mass ratios and mixings by powers of a small ‘hierarchy parameter’ η . The resulting structure of mass matrices also arises in compactifications of higher-dimensional field and string theories, where the parameter η is related to the location of matter fields in the compact dimensions or to vacuum expectation values of moduli fields (cf. [3]).

In this article we consider a Froggatt-Nielsen symmetry which commutes with the GUT group $SU(5)$, and which naturally explains the large $\nu_\mu - \nu_\tau$ mixing [4]. This symmetry implies a particular hierarchy pattern in the Majorana mass matrix for the light neutrinos,

$$m_\nu \propto \begin{pmatrix} \eta^2 & \eta & \eta \\ \eta & 1 & 1 \\ \eta & 1 & 1 \end{pmatrix}, \quad (1)$$

which can be regarded as a key element for our analysis. The predicted Dirac and Majorana neutrino mass matrices are also consistent with leptogenesis [5]. Despite these successes, the predictive power of the Froggatt-Nielsen mechanism is rather limited due to unknown $\mathcal{O}(1)$ coefficients in all entries of the mass matrices. For example, the considered model [5] can accommodate both a small as well as a large ‘solar’ mixing angle θ_{12} [4, 6]. To get an idea of the range of possible predictions for a given flavour structure, it is instructive to treat the $\mathcal{O}(1)$ parameters as random variables [7].

In the following we shall employ Monte-Carlo techniques to study quantitatively the dependence of yet undetermined, but soon testable parameters of the neutrino sector on the unknown $\mathcal{O}(1)$ factors of the mass matrices. Using the already measured neutrino masses and mixings as input, we find surprisingly sharp predictions which indicate a large value for the smallest mixing angle θ_{13} in accordance with recent results from T2K [8], Minos [9] and Double Chooz [10], a value for the lightest neutrino mass of $\mathcal{O}(10^{-3})$ eV and one Majorana phase in the mixing matrix peaked at $\alpha_{21} = \pi$.

ψ_i	$\mathbf{10}_3$	$\mathbf{10}_2$	$\mathbf{10}_1$	$\mathbf{5}_3^*$	$\mathbf{5}_2^*$	$\mathbf{5}_1^*$	$\mathbf{1}_3$	$\mathbf{1}_2$	$\mathbf{1}_1$	H_u	H_d	S
Q_i	0	1	2	a	a	$a+1$	b	c	d	0	0	0

Table 1: Froggatt-Nielsen charge assignments. From Ref. [5].

2 Masses and mixings in the lepton sector

As far as orders of magnitude are concerned, the masses of quarks and charged leptons approximately satisfy the relations

$$\begin{aligned}
m_t : m_c : m_u &\sim 1 : \eta^2 : \eta^4, \\
m_b : m_s : m_d &\sim m_\tau : m_\mu : m_e \sim 1 : \eta : \eta^3,
\end{aligned}
\tag{2}$$

with $\eta^2 \simeq 1/300$ for masses defined at the GUT scale. This mass hierarchy can be reproduced by a simple U(1) flavour symmetry. Grouping the standard model leptons and quarks into the SU(5) multiplets $\mathbf{10} = (q_L, u_R^c, e_R^c)$ and $\mathbf{5}^* = (d_R^c, l_L)$, the Yukawa interactions take the form

$$\mathcal{L}_Y = h_{ij}^{(u)} \mathbf{10}_i \mathbf{10}_j H_u + h_{ij}^{(e)} \mathbf{5}_i^* \mathbf{10}_j H_d + h_{ij}^{(\nu)} \mathbf{5}_i^* \mathbf{1}_j H_u + \frac{1}{2} h_i^{(n)} \mathbf{1}_i \mathbf{1}_i S + \text{c.c.}, \tag{3}$$

where $\mathbf{1} = \nu_R^c$ denote the charge conjugates of right-handed neutrinos and $i, j = 1 \dots 3$ are flavour indices. Note that the Yukawa matrix $h^{(n)}$ for the right-handed neutrinos can always be chosen to be real and diagonal. H_u , H_d and S are the Higgs fields for electroweak and $B - L$ symmetry breaking, i.e., their vacuum expectation values generate the Dirac masses of quarks and leptons and the Majorana masses for the right-handed neutrinos, respectively. In this setup, the Yukawa couplings are determined up to complex $\mathcal{O}(1)$ factors by assigning U(1) charges to the fermion and Higgs fields in Eq. (3),

$$h_{ij} \sim \eta^{Q_i + Q_j}. \tag{4}$$

With the charge assignment given in Tab. 1 the mass relations in Eq. (2) are reproduced. Additionally, perturbativity of the Yukawa couplings and constraints on $\tan \beta = \langle H_u \rangle / \langle H_d \rangle$ require $0 \leq a \leq 1$.

Masses

From Eq. (3) and Tab. 1 one obtains for the Dirac neutrino mass matrix m_D and the Majorana mass matrix of the right-handed neutrinos M ,

$$\frac{m_D}{v_{EW} \sin \beta} = h_{ij}^{(\nu)} \sim \eta^a \begin{pmatrix} \eta^{d+1} & \eta^{c+1} & \eta^{b+1} \\ \eta^d & \eta^c & \eta^b \\ \eta^d & \eta^c & \eta^b \end{pmatrix}, \quad \frac{M}{v_{B-L}} = h_{ij}^{(n)} \sim \begin{pmatrix} \eta^{2d} & 0 & 0 \\ 0 & \eta^{2c} & 0 \\ 0 & 0 & \eta^{2b} \end{pmatrix}, \quad (5)$$

with the electroweak and $B - L$ symmetry breaking vacuum expectation values $v_{EW} = \sqrt{\langle H_u \rangle^2 + \langle H_d \rangle^2}$ and $v_{B-L} = \langle S \rangle$, respectively. In the seesaw formula

$$m_\nu = -m_D \frac{1}{M} m_D^T, \quad (6)$$

the dependence on the right-handed neutrino charges drops out, and one finds for the light neutrino mass matrix,

$$m_\nu \sim \frac{v_{EW}^2 \sin^2 \beta}{v_{B-L}} \eta^{2a} \begin{pmatrix} \eta^2 & \eta & \eta \\ \eta & 1 & 1 \\ \eta & 1 & 1 \end{pmatrix}. \quad (7)$$

The charged lepton mass matrix is given by

$$\frac{m_e}{v_{EW} \cos \beta} = h_{ij}^{(e)} \sim \eta^a \begin{pmatrix} \eta^3 & \eta^2 & \eta \\ \eta^2 & \eta & 1 \\ \eta^2 & \eta & 1 \end{pmatrix}. \quad (8)$$

Note that the second and third row of the matrix m_e have the same hierarchy pattern. This is a consequence of the same flavour charge for the second and third generation of leptons, which is the origin of the large neutrino mixing. Hence, diagonalizing m_e can a priori give a sizable contribution to the mixing in the lepton sector.

Mixing

The lepton mass matrices are diagonalized by bi-unitary and unitary transformations, respectively,

$$V_L^T m_e V_R = m_e^{\text{diag}}, \quad U^T m_\nu U = m_\nu^{\text{diag}}, \quad (9)$$

with $V_L^\dagger V_L = V_R^\dagger V_R = U^\dagger U = 1$. From V_L and U one obtains the leptonic mixing matrix $U_{\text{PMNS}} = V_L^\dagger U$, which is parametrized as [11]

$$U_{\text{PMNS}} = \begin{pmatrix} c_{12}c_{13} & s_{12}c_{13}e^{i\frac{\alpha_{21}}{2}} & s_{13}e^{i(\frac{\alpha_{31}}{2}-\delta)} \\ -s_{12}c_{23} - c_{12}s_{23}s_{13}e^{i\delta} & (c_{12}c_{23} - s_{12}s_{23}s_{13}e^{i\delta})e^{i\frac{\alpha_{21}}{2}} & s_{23}c_{13}e^{i\frac{\alpha_{31}}{2}} \\ s_{12}s_{23} - c_{12}c_{23}s_{13}e^{i\delta} & (-c_{12}s_{23} - s_{12}c_{23}s_{13}e^{i\delta})e^{i\frac{\alpha_{21}}{2}} & c_{23}c_{13}e^{i\frac{\alpha_{31}}{2}} \end{pmatrix}, \quad (10)$$

with $c_{ij} = \cos \theta_{ij}$ and $s_{ij} = \sin \theta_{ij}$. Since the light neutrinos are Majorana fermions, all three phases are physical.

In the following we study the impact of the unspecified $\mathcal{O}(1)$ factors in the lepton mass matrices on the various parameters of the neutrino sector by using a Monte Carlo method, taking present knowledge on neutrino masses and mixings into account. Naively, one might expect large uncertainties in the predictions for the observables of the neutrino sector obtained in this setup. For instance, the neutrino mass matrix is calculated by multiplying three matrices, in which each entry comes with an unspecified $\mathcal{O}(1)$ factor, cf. Eq. (6). However, carrying out the analysis described below and calculating the 68% confidence intervals, we find that in many cases our results are sharply peaked, yielding a higher precision than only an order-of-magnitude estimate.

3 Random variables

Monte-Carlo study

The unknown $\mathcal{O}(1)$ coefficients of the Yukawa matrices $h^{(e)}$, $h^{(\nu)}$ and $h^{(n)}$ are constrained by the experimental data on neutrino masses and mixings, with the 3σ confidence ranges given by [11]:

$$\begin{aligned}
2.07 \times 10^{-3} \text{ eV}^2 &\leq |\Delta m_{\text{atm}}^2| \leq 2.75 \times 10^{-3} \text{ eV}^2, \\
7.05 \times 10^{-5} \text{ eV}^2 &\leq \Delta m_{\text{sol}}^2 \leq 8.34 \times 10^{-5} \text{ eV}^2, \\
0.75 &\leq \sin^2(2\theta_{12}) \leq 0.93, \\
0.88 &\leq \sin^2(2\theta_{23}) \leq 1.
\end{aligned}
\tag{11}$$

In the following we explicitly do not use the current bound on the smallest mixing angle ($\theta_{13} < 0.21$ at 3σ [11]). This allows us to demonstrate that nearly all values we obtain for θ_{13} automatically obey the experimental bound, cf. Fig. 1.

In a numerical Monte-Carlo study we generate random numbers to model the 39 real parameters of the three mass matrices.¹ The absolute values are taken to be uniformly distributed in $[10^{-1/2}, 10^{1/2}]$ on a logarithmic scale. The phases in $h^{(e)}$ and $h^{(\nu)}$ are

¹Nine complex $\mathcal{O}(1)$ factors in each $h^{(\nu)}$ and $h^{(e)}$, as well as three real $\mathcal{O}(1)$ factors in $h^{(n)}$. Note that here we are treating the low energy Yukawa couplings as random variables, which are related to the couplings at higher energy scales via renormalization group equations. However, we expect that the effect of this renormalization group running can essentially be absorbed into a redefinition of the effective scale \bar{v}_{B-L} , hence leaving the results presented in the following unchanged.

chosen to be uniformly distributed in $[0, 2\pi)$. In the following, we shall refer to those sets of coefficients which are consistent with the experimental constraints in Eq. (11) as hits.

In a preliminary run, we consider the neutrino mixing matrix U , with the effective scale $\bar{v}_{B-L} \equiv \eta^{-2a} v_{B-L} / \sin^2 \beta$ treated as random variable in the interval $[10^{-1/2}, 10^{1/2}] \times 10^{15}$ GeV. We find that the percentage of hits strongly peaks at $\bar{v}_{B-L} \simeq 1 \times 10^{15}$ GeV. This is interesting for two reasons. Firstly, it implies that given $0 \leq a \leq 1$, the high seesaw scale lies in the range 3×10^{12} GeV $\lesssim v_{B-L} / \sin^2 \beta \lesssim 1 \times 10^{15}$ GeV. Note that the upper part of this mass range is close the GUT scale, which is important for recent work on the connection of leptogenesis, gravitino dark matter and hybrid inflation [12]. Secondly, this result allows us to fix the parameter \bar{v}_{B-L} in the following computations without introducing a significant bias.

In the main run, for fixed \bar{v}_{B-L} , we include the mixing matrix V_L of the charged leptons to compute the full PMNS matrix. We require the mass ratios of the charged leptons to fulfill the experimental constraints up to an accuracy of 5% and allow for $1 \leq \tan \beta \leq 60$ to achieve the correct normalization of the charged lepton mass spectrum. Finally, imposing the 3σ constraints on the two large mixing angles of the full PMNS matrix, we find parameter sets of $\mathcal{O}(1)$ factors which yield mass matrices fulfilling the constraints in Eq. (11). Our final results are based on roughly 20 000 such hits. For each hit we calculate the observables in the neutrino sector as well as parameters relevant for leptogenesis. The resulting distributions are discussed below.

Statistical analysis

In our theoretical setup the relative frequency with which we encounter a certain value for an observable might indicate the probability that this value is actually realized within the large class of flavour models under study. In the following we shall therefore treat the distributions for the various observables as probability densities for continuous random variables. That is, our predictions for the respective observables represent best-guess estimates according to a probabilistic interpretation of the relative frequencies.

For each observable we would like to deduce measures for its central tendency and statistical dispersion from the respective probability distribution. Unfortunately, it is infeasible to fit all obtained distributions with one common template distribution. Such a procedure would lack a clear statistical justification, and it also appears impractical as the distributions that we obtain differ substantially in their shapes. We therefore choose a different approach. We consider the median of a distribution as its centre

and we use the 68 % ‘confidence’ interval around it as a measure for its spread. Of course, this range of the confidence interval is reminiscent of the 1σ range of a normal distribution.

More precisely, for an observable x with probability density f we will summarize its central tendency and variability in the following form [13],

$$x = \hat{x}_{\Delta_{\pm}^+}, \quad \Delta_{\pm} = x_{\pm} - \hat{x}. \quad (12)$$

Here, x_- and x_+ denote the 16 %- and 84 %-quantiles with respect to the density function f . The central value \hat{x} is the median of f and thus corresponds to its 50 %-quantile. All three values of x can be calculated from the quantile function Q ,

$$Q(p) = \inf \{x \in [x_{\min}, x_{\max}] : p \leq F(x)\}, \quad F(x) = \int_{x_{\min}}^x dt f(t), \quad (13)$$

where F stands for the cumulative distribution function of x . We then have:

$$x_- = Q(0.16), \quad \hat{x} = Q(0.50), \quad x_+ = Q(0.84). \quad (14)$$

Intuitively, the intervals from x_{\min} to x_- , \hat{x} , and x_+ respectively correspond to the x ranges into which 16 %, 50 % or 84 % of all hits fall. This is also illustrated in the histogram for $\sin^2 2\theta_{13}$ in Fig. 1. Moreover, we have included vertical lines into each plot to indicate the respective positions of x_- , \hat{x} , and x_+ .

In our case the median is a particularly useful measure of location. First of all, it is resistant against outliers and hence an appropriate statistic for such skewed distributions as we observe them. But more importantly, the average absolute deviation from the median is minimal in comparison to any other reference point. The median is thus the best guess for the outcome of a measurement if one is interested in being as close as possible to the actual result, irrespective of the sign of the error. On the technical side the definition of the median fits nicely together with our method of assessing statistical dispersion. The 68 % confidence interval as introduced above is just constructed in such a way that equal numbers of hits lie in the intervals from x_- to \hat{x} and from \hat{x} to x_+ , respectively. In this sense, our confidence interval represents a symmetric error with respect to the median.

As a test of the robustness of our results, we checked the dependence of our distributions on the precise choice of the experimental error intervals. The results presented here proved insensitive to these variations. For definiteness, we therefore stick to the

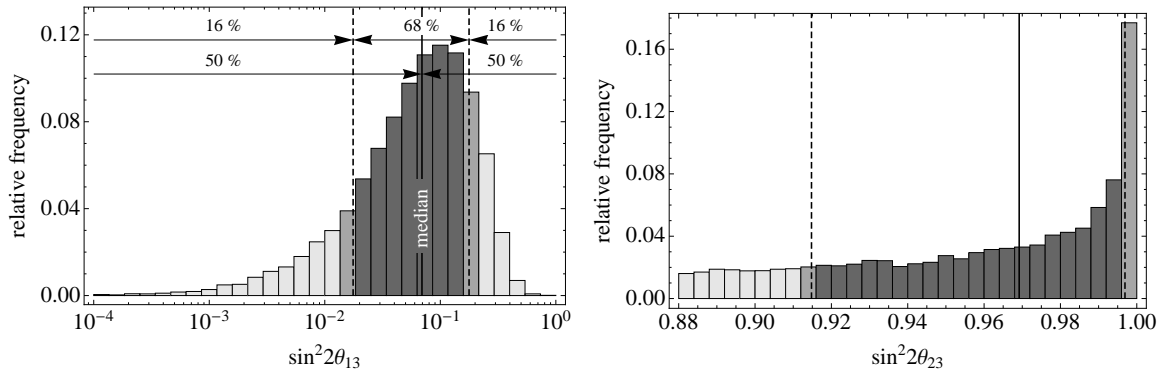


Figure 1: Neutrino mixing angles θ_{13} and θ_{23} . The vertical lines denote the position of the median (solid line) and the boundaries of the 68% confidence region (dashed lines) of the respective distribution.

3σ intervals. We also checked the effect of taking the random $\mathcal{O}(1)$ factors to be distributed uniformly on a linear instead of a logarithmic scale. Again, the results proved to be robust.

4 Observables and results

Mass hierarchy

An important open question which could help unravel the flavour structure of the neutrino sector is the mass hierarchy. Since the sign of Δm_{atm}^2 is not yet known, we cannot differentiate with current experimental data between a normal hierarchy with one heavy and two light neutrino mass eigenstates and an inverted hierarchy, which has two heavy and one light neutrino mass eigenstate. Measuring the Mikheyev-Smirnov-Wolfenstein (MSW) effect of the earth could resolve this ambiguity.

With the procedure described above, all hits match the structure of the normal hierarchy and there are no examples with inverted hierarchy. It is however notable that imposing the structure of the neutrino mass matrix given by Eq. (7) alone does not exclude the inverted mass hierarchy. Only additionally imposing the measured bounds on the mixing angles rejects this possibility.

Mixing angles

The mixing in the lepton sector is described by the matrix U_{PMNS} given in Eq. (10). Of the three angles, two are only bounded from one side by experiment: for the largest mixing angle θ_{23} there exists a lower bound, whereas the smallest mixing angle θ_{13}

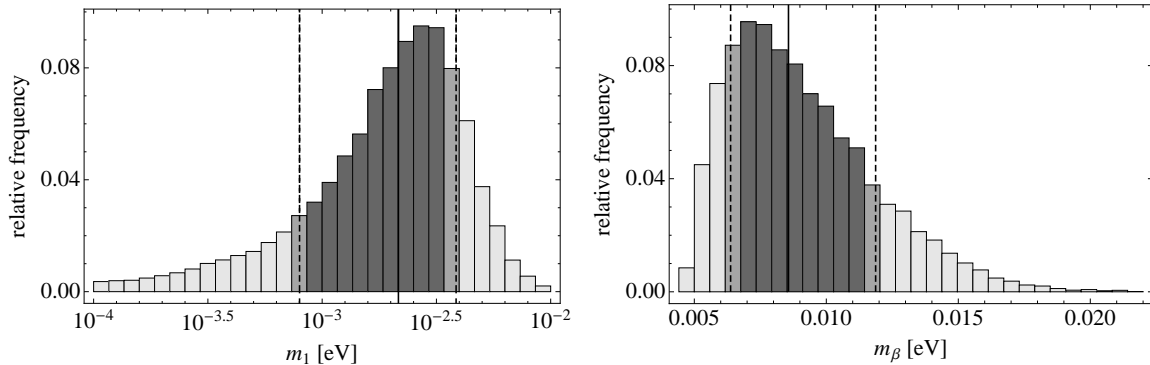


Figure 2: Lightest neutrino mass m_1 and effective neutrino mass in tritium decay m_β . Vertical lines and shadings as in Fig. 1.

is so far only bounded from above. Recent results from T2K [8], Minos [9] and the preliminary result of Double Chooz [10] point to a value of θ_{13} just below the current experimental bound. The respective best fit points, assuming a normal hierarchy, are $\sin^2 2\theta_{13} = 0.11$ (T2K), $2 \sin^2 \theta_{23} \sin^2 2\theta_{13} = 0.041$ (MINOS) and $\sin^2 2\theta_{13} = 0.085$ (Double Chooz). The 90% and 68% confidence regions respectively read

$$\begin{aligned}
0.03 < \sin^2 2\theta_{13} < 0.28 & & \text{T2K, 90 \% CL, } \delta_{CP} = 0, \\
2 \sin^2 \theta_{23} \sin^2 2\theta_{13} < 0.12 & & \text{MINOS, 90 \% CL, } \delta_{CP} = 0, \\
0.01 < \sin^2 2\theta_{13} < 0.16 & & \text{Double Chooz, 68 \% CL.}
\end{aligned} \tag{15}$$

With the procedure described above, we find sharp predictions for the smallest and the largest mixing angle within the current experimental bounds,

$$\sin^2 2\theta_{13} = 0.07_{-0.05}^{+0.11}, \quad \sin^2 2\theta_{23} = 0.97_{-0.05}^{+0.03}; \tag{16}$$

the corresponding distributions are shown in Fig. 1. These results are quite remarkable: the atmospheric mixing angle points to maximal mixing, while the rather large value for θ_{13} is consistent with the recent T2K, Minos and Double Chooz results.

In our Monte-Carlo study we observe that the dominant contribution to the strong mixing in the lepton sector is primarily due to the neutrino mass matrix m_ν . The numerical results are not much affected by including the charged lepton mixing matrix V_L . The PMNS matrix is thus approximately given by the matrix U which diagonalizes the light neutrino mass matrix m_ν .

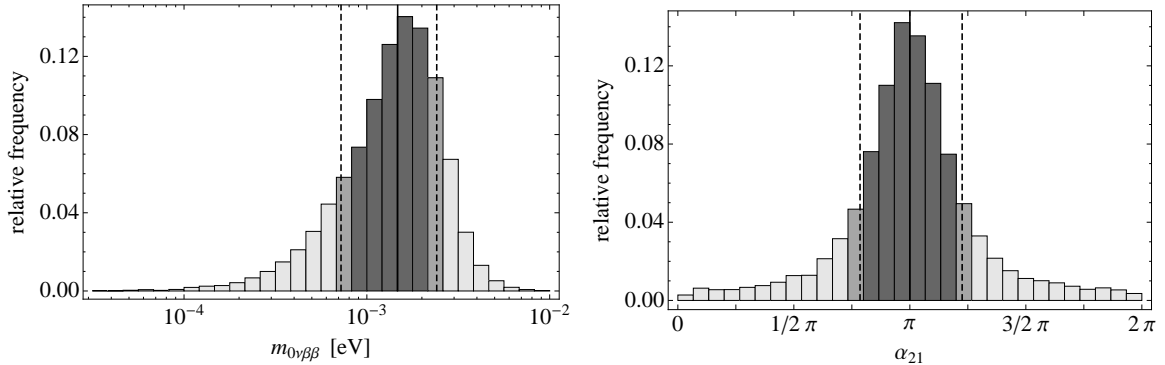


Figure 3: Effective mass in neutrinoless double-beta decay $m_{0\nu\beta\beta}$ and Majorana phase α_{21} . Vertical lines and shadings as in Fig. 1.

Absolute mass scale

The absolute neutrino mass scale is a crucial ingredient for the study of neutrinoless double-beta decay and leptogenesis. Although inaccessible in neutrino oscillation experiments, different experimental setups have succeeded in constraining this mass scale. Cosmological observations of the fluctuations in the cosmic microwave background, of the density fluctuations in the galaxy distribution and of the Lyman- α forest yield a constraint for the sum of the light neutrino masses, weighted by the number of spin degrees of freedom per Majorana neutrino, $g_\nu = 2$, [11]

$$m_{\text{tot}} = \sum_{\nu} \frac{g_\nu}{2} m_\nu \lesssim 0.5 \text{ eV}. \quad (17)$$

The Planck satellite is expected to be sensitive to values of m_{tot} as low as roughly 0.1 eV [14]. A further constraint arises from measuring the β -spectrum in tritium decay experiments. The current bound [11] is

$$m_\beta^2 = \sum_i |(U_{PMNS})_{ei}|^2 m_i^2 < 4 \text{ eV}^2. \quad (18)$$

By comparison, the KATRIN experiment, which will start taking data soon, aims at reaching a sensitivity of 0.04 eV^2 [15]. Finally, the neutrino mass scale can also be probed by neutrinoless double-beta decay. The relevant effective mass is

$$m_{0\nu\beta\beta} = \left| \sum_i (U_{PMNS})_{ei}^2 m_i \right|. \quad (19)$$

Here, Ref. [16] claims a value of $0.11 - 0.56 \text{ eV}$. Dedicated experiments, such as GERDA [17] with a design sensitivity of $0.09 - 0.20 \text{ eV}$, are on the way. Note that

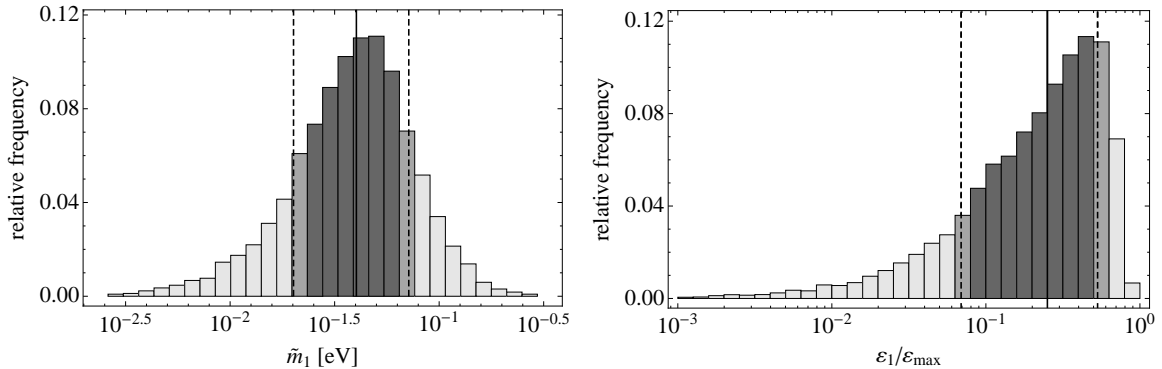


Figure 4: Effective neutrino mass of the first generation \tilde{m}_1 and CP violation parameter ε_1 . Vertical lines and shadings as in Fig. 1.

$m_{0\nu\beta\beta}$ does not only depend on the absolute neutrino mass scale and the mixing angles, but also on the phases ($\alpha_{31} - 2\delta$) and α_{21} in the PMNS matrix.

We find sharp predictions for the neutrino mass parameters discussed above. The lightest neutrino, ν_1 , is found to be quite light, cf. Fig. 2,

$$m_1 = 2.2^{+1.7}_{-1.4} \times 10^{-3} \text{ eV}, \quad (20)$$

hence favouring a relatively low neutrino mass scale beyond the reach of current and upcoming experiments. More precisely, we find for the neutrino mass parameters discussed above:

$$m_{\text{tot}} = 6.0^{+0.3}_{-0.3} \times 10^{-2} \text{ eV}, \quad m_\beta = 8.6^{+3.3}_{-2.2} \times 10^{-3} \text{ eV}, \quad m_{0\nu\beta\beta} = 1.5^{+0.9}_{-0.8} \times 10^{-3} \text{ eV}. \quad (21)$$

CP-violating phases

The small value of the mass parameter measured in neutrinoless double-beta decay, $m_{0\nu\beta\beta}$, is due to the relative minus sign between the m_1 and m_2 terms in Eq. (19), caused by a strong peak of the value for the Majorana phase α_{21} at π ,

$$\frac{\alpha_{21}}{\pi} = 1.0^{+0.2}_{-0.2}. \quad (22)$$

This is depicted in Fig. 3. An analytic analysis of how this phenomena arises from the structure of the neutrino mass matrix, cf. Eq. (7), is presented in Appendix A. For the other Majorana phase α_{31} and the Dirac phase δ we find no such distinct behaviour but approximately flat distributions.

Leptogenesis parameters

Finally, leptogenesis [18] links the low energy neutrino physics to the high energy physics of the early universe. The parameters that capture this connection are the effective neutrino mass of the first generation \tilde{m}_1 and the CP violation parameter ε_1 [19],

$$\tilde{m}_1 = \frac{(m_D^\dagger m_D)_{11}}{M_1}, \quad \varepsilon_1 = - \sum_{j=2,3} \frac{\text{Im} [(h^{(\nu)\dagger} h^{(\nu)})_{1j}]^2}{8\pi (h^{(\nu)\dagger} h^{(\nu)})_{11}} F\left(\frac{M_j^2}{M_1^2}\right), \quad (23)$$

with $F(x) = \sqrt{x} \left(\ln \frac{1+x}{x} + \frac{2}{x-1} \right)$ and M_j denoting the masses of the heavy neutrinos. Here, \tilde{m}_1 determines the coupling strength of the lightest of the heavy neutrinos to the thermal bath and thus controls the significance of wash-out effects. It is bounded from below by the lightest neutrino mass m_1 . The absolute value of the CP violation parameter ε_1 is bounded from above by [20]

$$\varepsilon_{\max} = \frac{3}{8\pi} \frac{|\Delta m_{\text{atm}}^2|^{1/2} M_1}{v_{EW}^2 \sin^2 \beta} \simeq 2.1 \times 10^{-6} \left(\frac{1}{\sin^2 \beta} \right) \left(\frac{M_1}{10^{10} \text{ GeV}} \right). \quad (24)$$

With the procedure described above, we find

$$\tilde{m}_1 = 4.0_{-2.0}^{+3.1} \times 10^{-2} \text{ eV}, \quad \frac{\varepsilon_1}{\varepsilon_{\max}} = 0.25_{-0.18}^{+0.28}, \quad (25)$$

and hence a clear preference for the strong wash-out regime [19]. Notice that there typically is a hierarchy between \tilde{m}_1 and m_1 of about one order of magnitude. The relative frequency of the CP violation parameter ε_1 peaks close to the upper bound ε_{\max} , with the majority of the hits lying within one order of magnitude or less below ε_{\max} , cf. Fig. 4. This justifies the use of ε_{\max} when estimating the produced lepton asymmetry in leptogenesis. Here, in the discussion of ε_1 , we assumed hierarchical heavy neutrinos, $M_{2,3} \gg M_1$.

Theoretical versus experimental input

The results of this section are obtained by combining two conceptually different inputs, on the one hand the hierarchy structure of the neutrino mass matrix m_ν given by Eq. (1) and on the other hand the experimentally measured constraints listed in Eq. (11). In general, the distributions presented above really arise from the interplay between both of these ingredients. For example, the hierarchy structure alone does not favour a large solar mixing angle θ_{12} and the ratio $\Delta m_{\text{sol}}^2 / \Delta m_{\text{atm}}^2$ tends to be too large (cf. [21, 22]). This discrepancy is eased by generating the random coefficients in Eq. (1) via the seesaw mechanism. Imposing the experimental constraints finally singles out the subset

of parameter sets used for the distributions presented above. As another example, consider the smallest mixing angle θ_{13} and the lightest neutrino mass eigenstate m_1 . In these cases, the hierarchy structure of the neutrino mass matrix automatically implies small values, similar to those shown in the distributions above. However, the exact distributions including the precise position of the peaks only arise after implementing the experimental constraints. A notable exception to this scheme is the Majorana phase α_{21} . Here the peak at $\alpha_{21} = \pi$ is a result of the hierarchy structure of the neutrino matrix m_ν alone, as demonstrated in Appendix A.

5 Discussion and outlook

In summary, we find that starting from a flavour symmetry which accounts for the measured quark and lepton mass hierarchies and large neutrino mixing, the present knowledge of neutrino parameters strongly constrains the yet unknown observables, in particular the smallest mixing angle θ_{13} , the smallest neutrino mass m_1 , and the Majorana phase α_{21} . This statement is based on a Monte-Carlo study: Treating unspecified $\mathcal{O}(1)$ parameters of the considered Froggatt-Nielsen model as random variables, the observables of interest are sharply peaked around certain central values.

We expect that these results hold beyond Froggatt-Nielsen flavour models. An obvious example are extradimensional models which lead to the same type of light neutrino mass matrix (cf. [23]). On the other hand, quark-lepton mass hierarchies and the presently known neutrino observables cannot determine the remaining observables in a model-independent way. This is illustrated by the fact that our present knowledge about quark and lepton masses and mixings is still consistent with $\theta_{13} \simeq 0$ as well as with an inverted neutrino mass hierarchy (cf. [24]). As a consequence, further measurements of neutrino parameters will be able to falsify certain patterns of flavour mixing and thereby provide valuable guidance for the theoretical origin of quark and lepton mass matrices.

Acknowledgements

The authors thank G. Altarelli, F. Brümmer, G. Ross, D. Wark, W. Winter and T. Yanagida for helpful discussions and comments. This work has been supported by the German Science Foundation (DFG) within the Collaborative Research Center 676 “Particles, Strings and the Early Universe”.

A Analytic derivation of the Majorana phase α_{21}

The complex phases of the $\mathcal{O}(1)$ coefficients in the neutrino mass matrix m_ν and the lepton mass matrix m_e are randomly distributed. One would thus naively expect that also the Majorana phases α_{21} and α_{31} in the PMNS matrix can take arbitrary values. By contrast, the distribution of values for α_{21} that we obtain from our numerical Monte-Carlo study, cf. Fig. 3, clearly features a prominent peak at $\alpha_{21} = \pi$. In this appendix we shall demonstrate by means of a simplified example how the structure of the neutrino mass matrix m_ν may partly fix the phases of the corresponding mixing matrix U .

Consider the following simplified Majorana mass matrix m_ν for the light neutrinos,

$$m_\nu = v \begin{pmatrix} \eta^2 & \eta e^{i\varphi} & \eta \\ \eta e^{i\varphi} & 1 & 1 \\ \eta & 1 & 1 \end{pmatrix}, \quad v = \frac{v_{\text{EW}}^2}{\bar{v}_{B-L}}, \quad (26)$$

where φ is an arbitrary complex phase between 0 and 2π . For simplicity, let us neglect any effects on the mixing matrix U from the diagonalization of m_e . That is, we define U such that $U^T m_\nu U = \text{diag}(m_i)$, with m_i^2 denoting the eigenvalues of $m_\nu^\dagger m_\nu$,

$$\begin{aligned} \frac{m_{1,2}^2}{v^2} &= \eta^2 \sin^2(\varphi/2) \left[2 \mp \eta (5 + 3 \cos(\varphi))^{1/2} \right] + \mathcal{O}(\eta^4), \\ \frac{m_3^2}{v^2} &= 4 (1 + \eta^2 [1 - \sin^2(\varphi/2)]) + \mathcal{O}(\eta^4). \end{aligned} \quad (27)$$

Notice that the first two mass eigenvalues are nearly degenerate. This is a consequence of the particular hierarchy pattern of the matrix m_ν which originally stems from the equal flavour charges of the $\mathbf{5}_2^*$ and $\mathbf{5}_3^*$ multiplets. The relative sign of the $\mathcal{O}(\eta^3)$ contributions to m_1^2 and m_2^2 eventually shows up again in entries of U , for instance,

$$U_{11,12} = \mp \frac{2(5 + 3 \cos(\varphi))^{1/2}}{3 + e^{i\varphi}} \exp\left(-\frac{i}{2} \text{Arg}[\mp z]\right) + \mathcal{O}(\eta). \quad (28)$$

with $z = 1 - \cos(\varphi) - 2i \sin(\varphi)$. The phase $\alpha_{21} = 2(\text{Arg}[U_{12}/U_{11}] \bmod \pi)$ in the matrix U represents the analog of the Majorana phase α_{21} in the PMNS matrix, cf. Eq. (10). According to our explicit results for U_{11} and U_{12} it is independent of the arbitrary phase φ to leading order in η ,

$$\alpha_{21} \simeq 2 \left(\text{Arg} \left[-\exp\left(-\frac{i}{2} \text{Arg}[+z] + \frac{i}{2} \text{Arg}[-z]\right) \right] \bmod \pi \right) = \pi. \quad (29)$$

In a similar way we may determine the phase analogous to the Majorana phase α_{31} . However, due to the hierarchy between the mass eigenvalues m_1 and m_3 , the first and third column of the matrix U differ significantly from each other, thus leading to a phase that depends on φ at all orders of η .

Including corrections to all orders in η and scanning over the phase φ numerically shows that the maximal possible deviation of α_{21} from π is, in fact, of order η^4 . Adding more complex phases to the matrix m_ν in Eq. (26) gradually smears out the peak in the distribution of α_{21} values. The distribution that is reached in the case of six different phases is already very similar to the one in Fig. 3. We conclude that despite the need for corrections the rough picture sketched in this appendix remains valid: The hierarchy pattern of the neutrino mass matrix directly implies that α_{21} tends to be close to $\alpha_{21} = \pi$.

References

- [1] For a review and references see, for example, S. Raby, Eur. Phys. J. C **59**, 223 (2009)
- [2] C. D. Froggatt and H. B. Nielsen, Nucl. Phys. B **147**, 277 (1979)
- [3] Y. Grossman and M. Neubert, Phys. Lett. B **474**, 361 (2000); T. Gherghetta and A. Pomarol, Nucl. Phys. B **586**, 141 (2000); W. Buchmuller, K. Hamaguchi, O. Lebedev and M. Ratz, Nucl. Phys. B **785**, 149 (2007)
- [4] J. Sato and T. Yanagida, Phys. Lett. B **430**, 127 (1998); N. Irges, S. Lavignac and P. Ramond, Phys. Rev. D **58**, 035003 (1998)
- [5] W. Buchmuller and T. Yanagida, Phys. Lett. B **445**, 399 (1999)
- [6] F. Vissani, JHEP **9811**, 025 (1998)
- [7] L. J. Hall, H. Murayama and N. Weiner, Phys. Rev. Lett. **84**, 2572 (2000); J. Sato and T. Yanagida, Phys. Lett. B **493**, 356 (2000); F. Vissani, Phys. Lett. B **508**, 79 (2001)
- [8] K. Abe *et al.* [T2K Collaboration], Phys. Rev. Lett. **107**, 041801 (2011)
- [9] P. Adamson *et al.* [MINOS Collaboration], Phys. Rev. Lett. **107**, 181802 (2011).

- [10] Talk given by H. de Kerret at the Sixth International Workshop on Low Energy Neutrino Physics (LowNu11) at Seoul, Korea during November 9-12, 2011
- [11] K. Nakamura *et al.* [Particle Data Group], *J. Phys. G* **37**, 075021 (2010)
- [12] W. Buchmuller, K. Schmitz and G. Vertongen, *Phys. Lett. B* **693**, 421 (2010);
W. Buchmuller, K. Schmitz and G. Vertongen, *Nucl. Phys. B* **851**, 481 (2011);
W. Buchmuller, V. Domcke and K. Schmitz, arXiv:1202.6679 [hep-ph].
- [13] G. Cowan, “Statistical data analysis,” Oxford, UK: Clarendon (1998) 197 p
- [14] [Planck Collaboration], ESA-SCI(2005)1 (2006), arXiv:astro-ph/0604069
- [15] M. Beck [KATRIN Collaboration], *J. Phys. Conf. Ser.* **203** (2010) 012097
- [16] H. V. Klapdor-Kleingrothaus, A. Dietz, H. L. Harney, I. V. Krivosheina, *Mod. Phys. Lett.* **A16**, 2409-2420 (2001)
- [17] G. Meierhofer [GERDA Collaboration], *J. Phys. Conf. Ser.* **312** (2011) 072011.
- [18] M. Fukugita, T. Yanagida, *Phys. Lett.* **B174**, 45 (1986).
- [19] For reviews containing the relevant formulae see, for example,
W. Buchmuller, R. D. Peccei and T. Yanagida, *Ann. Rev. Nucl. Part. Sci.* **55**, 311 (2005); S. Davidson, E. Nardi and Y. Nir, *Phys. Rept.* **466**, 105 (2008)
- [20] S. Davidson and A. Ibarra, *Phys. Lett. B* **535**, 25 (2002); see also K. Hamaguchi, H. Murayama and T. Yanagida, *Phys. Rev. D* **65**, 043512 (2002)
- [21] G. Altarelli, F. Feruglio and I. Masina, *JHEP* **0301**, 035 (2003); I. Masina and C. A. Savoy, *Phys. Rev. D* **71**, 093003 (2005) [hep-ph/0501166].
- [22] F. Plentinger, G. Seidl and W. Winter, *Phys. Rev. D* **76**, 113003 (2007);
F. Plentinger, G. Seidl and W. Winter, *Nucl. Phys. B* **791**, 60 (2008)
- [23] T. Asaka, W. Buchmuller, L. Covi, *Phys. Lett.* **B563**, 209-216 (2003)
- [24] For a review and references see, for example,
G. Altarelli, F. Feruglio, *Rev. Mod. Phys.* **82**, 2701-2729 (2010); H. Ishimori, T. Kobayashi, H. Ohki, Y. Shimizu, H. Okada, M. Tanimoto, *Prog. Theor. Phys. Suppl.* **183**, 1-163 (2010)